Please cite this article in press as: Wu et al., Increased Mammalian Lifespan and a Segmental and Tissue-Specific Slowing of Aging after Genetic Reduction of mTOR Expression, Cell Reports (2013), http://dx.doi.org/10.1016/j.celrep.2013.07.030

Cell Reports
Report

Cell PRESS
Open ACCESS

Increased Mammalian Lifespan and a Segmental and Tissue-Specific Slowing of Aging after Genetic Reduction of mTOR Expression

J. Julie Wu,[1] Jie Liu,[1] Edmund B. Chen,[1] Jennifer J. Wang,[1] Liu Cao,[5] Nisha Narayan,[1] Marie M. Fergusson,[1] Ilsa I. Rovira,[1] Michele Allen,[2] Danielle A. Springer,[2] Cory U. Lago,[1] Shuling Zhang,[3] Wendy DuBois,[3] Theresa Ward,[6] Rafael deCabo,[6] Oksana Gavrilova,[4] Beverly Mock,[3] and Toren Finkel[1,*]
[1]Center for Molecular Medicine, National Heart, Lung and Blood Institute
[2]Murine Phenotyping Core, National Heart, Lung and Blood Institute
[3]Laboratory of Cancer Biology and Genetics, National Cancer Institute
[4]Mouse Metabolism Core, National Institute of Diabetes and Digestive and Kidney Diseases
National Institutes of Health, Bethesda, MD 20892, USA
[5]Key Laboratory of Medical Cell Biology, China Medical University, Shenyang 110001, China
[6]Translational Gerontology Branch, National Institute of Aging, National Institutes of Health, Baltimore, MD 21224, USA
*Correspondence: finkelt@nih.gov
http://dx.doi.org/10.1016/j.celrep.2013.07.030
This is an open-access article distributed under the terms of the Creative Commons Attribution License, which permits unrestricted use, distribution, and reproduction in any medium, provided the original author and source are credited.

SUMMARY

We analyzed aging parameters using a mechanistic target of rapamycin (mTOR) hypomorphic mouse model. Mice with two hypomorphic (mTOR$^{\Delta/\Delta}$) alleles are viable but express mTOR at approximately 25% of wild-type levels. These animals demonstrate reduced mTORC1 and mTORC2 activity and exhibit an approximately 20% increase in median survival. While mTOR$^{\Delta/\Delta}$ mice are smaller than wild-type mice, these animals do not demonstrate any alterations in normalized food intake, glucose homeostasis, or metabolic rate. Consistent with their increased lifespan, mTOR$^{\Delta/\Delta}$ mice exhibited a reduction in a number of aging tissue biomarkers. Functional assessment suggested that, as mTOR$^{\Delta/\Delta}$ mice age, they exhibit a marked functional preservation in many, but not all, organ systems. Thus, in a mammalian model, while reducing mTOR expression markedly increases overall lifespan, it affects the age-dependent decline in tissue and organ function in a segmental fashion.

INTRODUCTION

Inhibiting target of rapamycin (TOR) activity appears to extend lifespan in various model systems, including yeast, worms, and flies (Bjedov et al., 2010; Kaeberlein et al., 2005; Kapahi et al., 2004; Medvedik et al., 2007; Vellai et al., 2003). Moreover, deletion of the TOR1 gene in yeast results in an increase in replicative lifespan that cannot be further extended by nutrient restriction (Kaeberlein et al., 2005). Evidence also suggests that mechanistic TOR (mTOR) plays a role in regulating mammalian lifespan. Treatment of mice beginning at 20 months of age with rapamycin, a pharmacological inhibitor of mTOR, results in an extension of lifespan that averages 9% for males and 13% for females (Harrison et al., 2009). When rapamycin was initiated at 9 months of age, median survival was increased to 10% for males and 18% for females (Miller et al., 2011). Similarly, deletion of ribosomal S6 protein kinase 1 (S6K1), a downstream effector of mTOR, extends the median lifespan of female S6K1$^{-/-}$ mice by approximately 19% (Selman et al., 2009). Very recently, an additional genetic model consisting of mice heterozygous for deletion of both mTOR and mLST8 (mammalian lethal with Sec13 protein 8) also demonstrated lifespan extension, again only evident in female mice (Lamming et al., 2012).

In mammals, mTOR exists in two distinct complexes, termed mTORC1 and mTORC2. Each of these mTOR complexes has distinct protein components, although both share the catalytic mTOR subunit, as well as mLST8 (Dazert and Hall, 2011; Laplante and Sabatini, 2012; Zoncu et al., 2011). Agents such as rapamycin are known to acutely inhibit mTORC1, although chronic treatment can also affect the activity of mTORC2 (Lamming et al., 2012; Sarbassov et al., 2006). How reducing mTOR activity extends lifespan remains incompletely understood. In addition, whether manipulations of pathways that regulate mammalian lifespan will slow aging and age-related pathologies in a uniform or segmental fashion remains largely unexplored. Here, using a genetic model of reduced mTOR expression, we provide evidence that reducing mTOR activity produces a marked increase in overall lifespan while also regulating an important, but not universal, subset of tissue-specific, age-dependent parameters.

RESULTS

Reduced mTOR Expression Increases Survival

To assess the role of mTOR in mammalian aging, we used a model of hypomorphic mTOR expression that has been recently

Cell PRESS
Open ACCESS

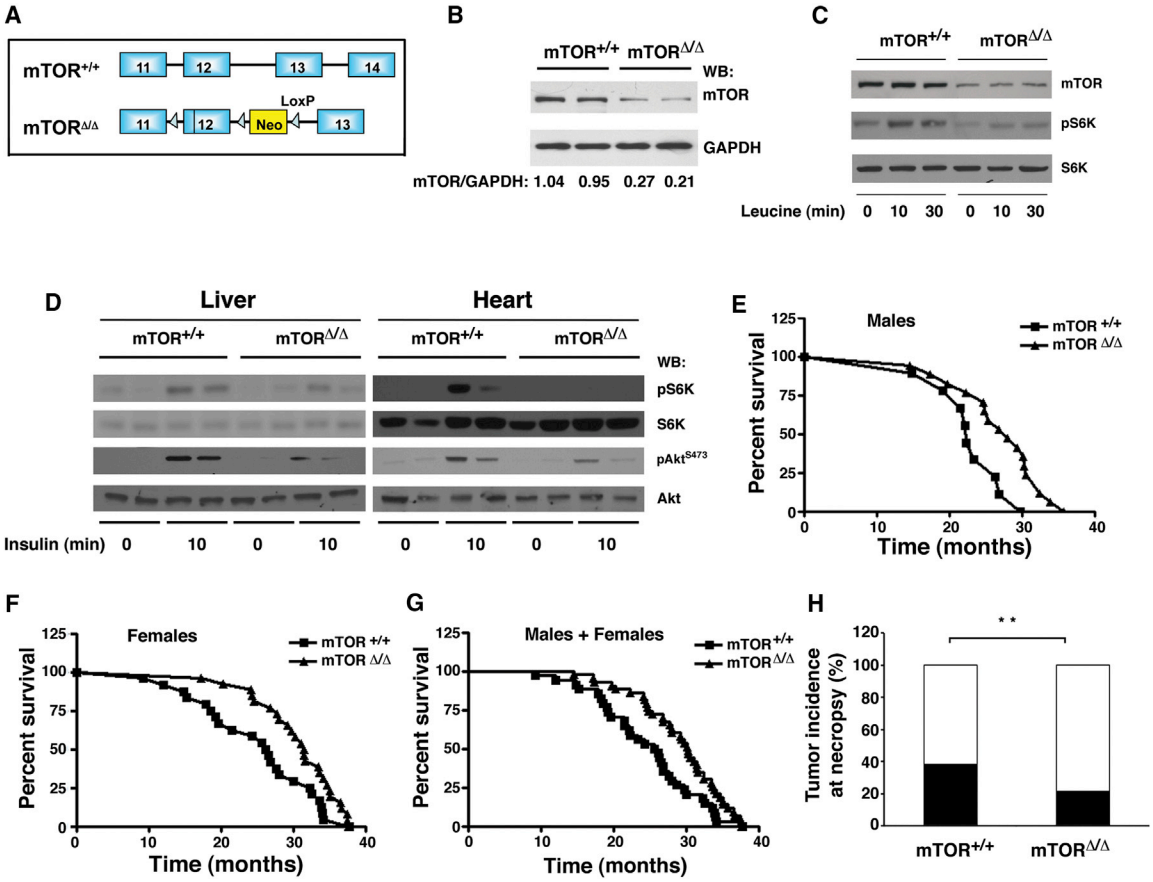

Figure 1. A Mouse Model of Reduced mTOR Expression Extends Life Span

(A) Genomic Organization of the WT Allele (+) and the Hypomorphic mTOR Allele (Δ).

(B) Representative mTOR protein expression in the liver of two WT ($mTOR^{+/+}$) and two $mTOR^{\Delta/\Delta}$ mice. GAPDH is used as a loading control, and the normalized expression (WT = 1) of mTOR to GAPDH is shown for each mouse.

(C) Leucine-stimulated S6 Kinase phosphorylation (pS6K) in primary mouse embryonic fibroblasts isolated from WT or $mTOR^{\Delta/\Delta}$ mice.

(D) Insulin-stimulated mTOR activity in pairs of WT or $mTOR^{\Delta/\Delta}$ mice.

(E) Survival of a cohort of male WT and $mTOR^{\Delta/\Delta}$ mice.

(F) Survival of female members of the cohort.

(G) Survival of the overall cohort.

(H) Incidence of malignant tumors found at necropsy denoted by shaded portion of each bar. While the overall incidence of cancer was different between the two genotypes, the spectrum of tumors observed was similar. $^{**}p < 0.001$, Fisher's exact test.

See also Figure S1.

described (Zhang et al., 2011). This model results from a floxed neomycin cassette inserted between exons 12 and 13 of the mTOR locus that results in the partial disruption of mTOR transcription (Figure 1A). While complete disruption of Raptor, Rictor, mLST8, or mTOR is embryonically lethal (Gangloff et al., 2004; Guertin et al., 2006; Murakami et al., 2004), $mTOR^{\Delta/\Delta}$ mice were viable in a mixed 129/C57BL/6 background. Analysis of tissues derived from $mTOR^{\Delta/\Delta}$ mice revealed that the level of mTOR protein was reduced to approximately 25% of wild-type (WT) levels (Figures 1B and S1A). Mouse embryonic fibroblasts (MEFs) derived from $mTOR^{\Delta/\Delta}$ mice also exhibited reduced mTOR expression, with no apparent alteration in the expression of associated proteins such as Raptor and Rictor (Figures 1C and S1B). When MEFs derived from $mTOR^{\Delta/\Delta}$ mice were analyzed, levels of TORC1 and TORC2 complexes appeared to be reduced to a similar degree (Figure S1B). As expected, $mTOR^{\Delta/\Delta}$ MEFs had reduced activation of S6 kinase following leucine addition (Figure 1C), although the overall level of protein translation was not altered (Figure S1C). We noted that $mTOR^{\Delta/\Delta}$ mice also exhibited a decrease in mTOR signaling in vivo. In particular, the activation of S6 kinase following insulin administration was markedly attenuated in $mTOR^{\Delta/\Delta}$ mice (Figure 1D). Similarly, the mTORC2 dependent serine 473 phosphorylation of Akt was also reduced in these mice.

We next asked whether this reduction in mTOR activity was sufficient to provide an extension in lifespan. Median survival of the $mTOR^{\Delta/\Delta}$ male mice was significantly higher than observed in $mTOR^{+/+}$ (WT) male mice (Figure 1E; median survival for WT, 22.9 months [n = 10]; for $mTOR^{\Delta/\Delta}$, 28.0 months [n = 17]; 22% extension, p = 0.02 by log rank [Mantel-Cox] test). Similarly,

Cell PRESS
Open ACCESS

the observed median survival for WT female mice was 26.5 months (n = 24), whereas for female mTOR$^{\Delta/\Delta}$ mice (n = 26), median survival was 31.5 months (Figure 1F; 19% extension, p = 0.047 by log rank test). For the overall combined cohort, median survival was 26.2 months for WT mice and 30.3 months for mTOR$^{\Delta/\Delta}$ mice (n = 34 for mTOR$^{+/+}$ mice and n = 43 for mTOR$^{\Delta/\Delta}$ mice, p = 0.0057 by Cox regression using sex and genotype as predictors; Figure 1G). We also assessed whether mTOR$^{\Delta/\Delta}$ mice had an increase in maximal lifespan by using the number of mice in each group that were still alive after 90% of the pooled distribution of WT and the mTOR$^{\Delta/\Delta}$ mice were dead (Wang et al., 2004). Of the 77 mice in the total cohort, 8 met this criteria, of which 1 was WT and 7 were mTOR$^{\Delta/\Delta}$ mice (p = 0.071, Fisher's exact test; and p = 0.061 when both genotype and sex were used as predictors). A similar analysis using an 80th percentile cutoff demonstrated that, with this less restrictive threshold, mTOR$^{\Delta/\Delta}$ mice exhibited an increase in maximal lifespan (p = 0.005, using genotype and sex as predictors).

Mice involved in the lifespan analysis were not subject to any physiological testing and received no treatment except if they developed a visible superficial infection. In such cases, the facility staff provided a short course of oral, subcutaneous, or topical antibiotics with or without ibuprofen (5 of 34 WT and 10 of 43 mTOR$^{\Delta/\Delta}$ mice received some treatment). If the infection persisted or worsened, to the point the mouse was felt to be in significant pain or functionally impaired, then the mouse was euthanized. In some older mice, the initial superficial infection was not discovered until it had progressed to such a degree that the staff believed the condition was too severe to respond to standard treatment, and, as such, the animal was euthanized without any prior treatment. We noted that the percentage of mice euthanized because of severe or progressive superficial infections was much higher in the mTOR$^{\Delta/\Delta}$ mice cohort (WT mice = 17%, and mTOR$^{\Delta/\Delta}$ mice = 37%; p < 0.01, Fisher's exact test). In contrast, mTOR$^{\Delta/\Delta}$ mice demonstrated an apparent reduction in the incidence of malignant tumors found at necropsy (Figures 1H, S1D, and S1E; 10 of 26 WT mice [38.5%] sent to necropsy versus 8 of 36 [21%] mTOR$^{\Delta/\Delta}$ mice sent to necropsy; **p < 0.01, Fisher's exact test). Besides the observed change in rates of malignancies and infections, there were no other marked differences in postmortem pathologies observed between WT and mTOR$^{\Delta/\Delta}$ mice.

No Alterations in Glucose Homeostasis or Metabolism in the mTOR$^{\Delta/\Delta}$ Mice

Analysis of body size (Figure 2A) and body weight (Figure 2B) revealed that mTOR$^{\Delta/\Delta}$ mice were consistently smaller than their WT littermates, although normalized body composition was unchanged (Figure S2A). When food intake was normalized to body weight, mTOR$^{\Delta/\Delta}$ mice and WT mice consumed equivalent amount of calories (Figure 2C). While rapamycin treatment in mice results in alteration in glucose homeostasis (Cunningham et al., 2007; Lamming et al., 2012), analysis of young mTOR$^{\Delta/\Delta}$ mice revealed no significant alterations in glucose tolerance (Figure 2D) or insulin sensitivity (Figure 2E). Indeed, while a reduction in insulin signaling is associated with increased lifespan (Kenyon, 2011), fasting levels of insulin were slightly higher in the mTOR$^{\Delta/\Delta}$ mice (Figure S2B). This appeared to relate in part to a cell-autonomous increase in insulin secretion from pancreatic islets isolated from mTOR$^{\Delta/\Delta}$ mice (Figures S2C and S2D). Analysis of older WT and mTOR$^{\Delta/\Delta}$ mice revealed that there was also no marked difference in glucose tolerance as these mice aged (Figure S2E). Serum analysis revealed no significant differences in various lipid parameters (Figures S2F, S2G, and S2H). Finally, the respiratory exchange ratio (Figure 2F), in vivo fatty acid oxidation rates (Figure 2G), the overall metabolic rate (Figure 2H), and normalized energy expenditure (Figure 2I) were all unaltered in mTOR$^{\Delta/\Delta}$ mice. Thus, as previously observed, the lifespan extension observed by reducing mTOR expression does not appear to result from a significant alteration in energetic or metabolic parameters (Lamming et al., 2012).

Biomarkers of Aging Are Reduced in the mTOR$^{\Delta/\Delta}$ Mice

When compared to a cohort of young mice, we observed a significant increase in p16^{Ink4A} mRNA in the tissues of old WT mice (Krishnamurthy et al., 2004). This age-dependent increase in p16^{Ink4a} mRNA was significantly reduced when kidneys and livers of aged matched mTOR$^{\Delta/\Delta}$ mice were assessed (Figures 3A and 3B). Aging tissues also exhibit evidence of increased oxidative stress and accumulation of protein aggregates (Kastle and Grune, 2011; Schöneich, 2006; Shang and Taylor, 2011). As previously described (Schöneich, 2006), when compared to young WT mice, tissues from old WT mice exhibited a marked increase in nitrotyrosine staining (Figures 3C, S3A, and S3B). When compared to age-matched WT mice, old mTOR$^{\Delta/\Delta}$ mice had significantly reduced levels of tissue nitrotyrosine staining (Figures 3C and 3D). Older tissues also accumulate aggregates of polyubiquitinated proteins (Kastle and Grune, 2011). These proteins are cleared in part by the mTOR-regulated process of autophagy. Older tissues of WT mice demonstrated a clear increase in the accumulation of polyubiquitin proteins, and this accumulation was less evident in mTOR$^{\Delta/\Delta}$ tissues (Figures 3E, 3F, S3C, and S3D).

mTOR$^{\Delta/\Delta}$ Mice Have Selective Improvement in Tissue and Organ Aging

We next sought to evaluate a variety of age-dependent parameters that might be important determinants of improved quality of life, independent of median lifespan. We first evaluated spatial learning and memory using the Barnes maze test, a noninvasive assessment of hippocampal function (Kennard and Woodruff-Pak, 2011). We noted no differences in the latency time to find the escape hole between young WT and mTOR$^{\Delta/\Delta}$ mice (Figure 4A). Latency times significantly increased in old WT mice, consistent with the well-known age-dependent decline in spatial learning and memory. While latency times also increased in old mTOR$^{\Delta/\Delta}$ mice, this age-dependent impairment was significantly less than what was observed in WT mice. By manually tracking the mice, we could also assess the learning strategies used during the training period. In both young and old mice, initially mice seek the escape hole using a random strategy. Over time, as spatial memory is encoded, the approach becomes more serial and directed. The amount of training required to have the latter strategy predominate (indicated by the colored arrows in Figure 4B) was approximately 1 day longer in old WT mice compared to old mTOR$^{\Delta/\Delta}$ mice). This is consistent with old

Cell PRESS
Open ACCESS

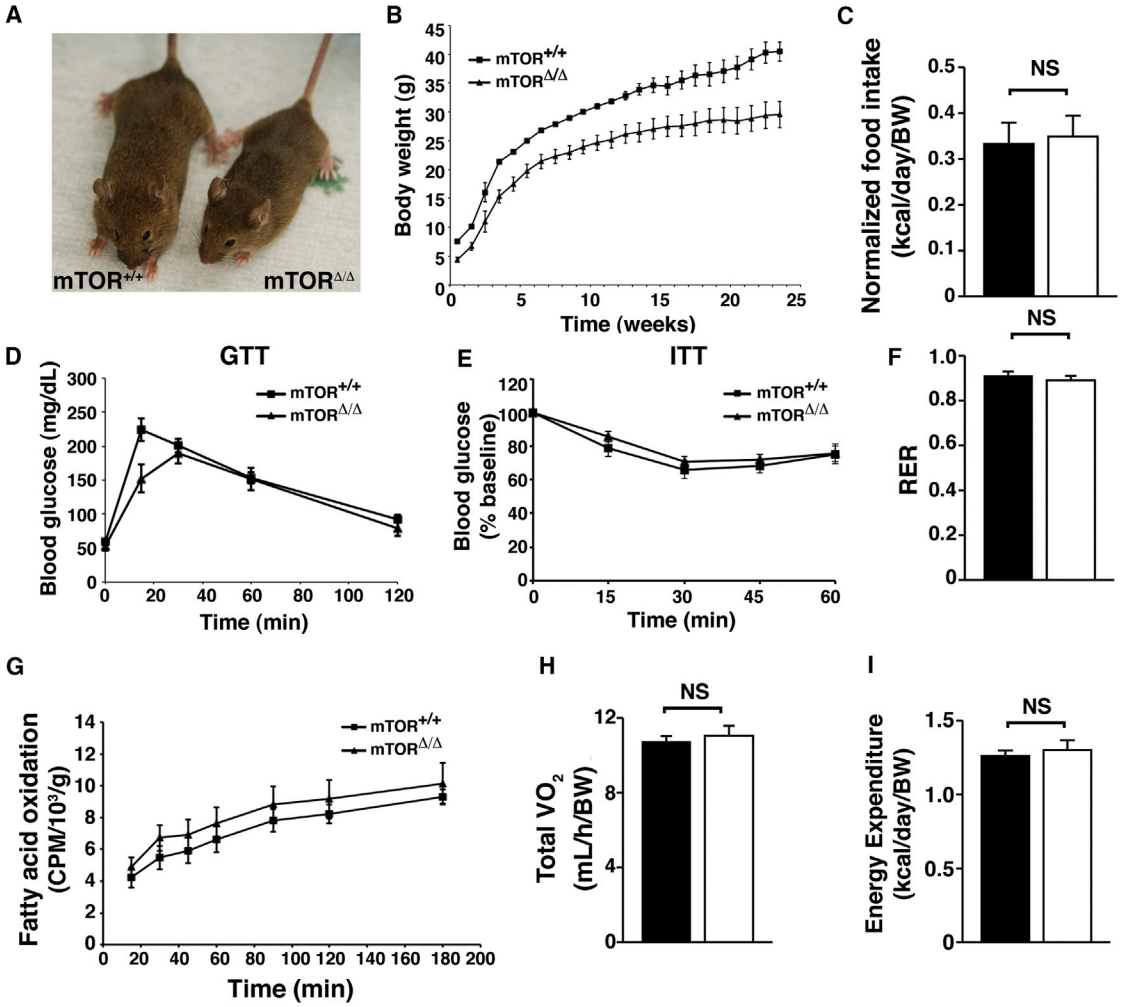

Figure 2. The mTOR$^{\Delta/\Delta}$ Mice Are Smaller but Have No Significant Alterations in Glucose Homeostasis and Metabolism

All measurements were performed using male mice.

(A) Representative size of a WT mouse and an mTOR$^{\Delta/\Delta}$ adult mouse.

(B) Body weight of WT (n = 7) and mTOR$^{\Delta/\Delta}$ (n = 7). Curves are statistically different using a one-way analysis of variance followed by two-tailed t test, $p < 0.01$.

(C) Daily food intake is indistinguishable between WT mice (shaded bar) and mTOR$^{\Delta/\Delta}$ mice (open bar) (n = seven WT mice, and n = six mTOR$^{\Delta/\Delta}$ mice; food intake is normalized to body weight).

(D) Glucose tolerance of 8- to 12-week-old WT (n = 7) and mTOR$^{\Delta/\Delta}$ (n = 6) mice.

(E) Insulin tolerance test of 8- to 12-week-old WT (n = 12) and mTOR$^{\Delta/\Delta}$ (n = 7) mice.

(F) Respiratory exchange ratio (RER) of WT (n = 7) and mTOR$^{\Delta/\Delta}$ (n = 5) mice.

(G) Measurement of rates of total body fatty acid oxidation normalized to body weight in WT (n = 7) and mTOR$^{\Delta/\Delta}$ (n = 5).

(H) Total oxygen consumption normalized to body weight (n = WT and n = 5 mTOR$^{\Delta/\Delta}$ mice).

(I) Total daily energy expenditure is not altered in mTOR$^{\Delta/\Delta}$ mice (n = seven WT mice and n = five mTOR$^{\Delta/\Delta}$ mice). For all panels, shaded bars represent the WT mice, and the open bars represent the mTOR$^{\Delta/\Delta}$ mice. Where indicated, metabolic parameters are adjusted to body weight raised to the 0.75 power, as indicated by the symbol (BW).

All pooled data are presented as mean ± SEM. See also Figure S2.

mTOR$^{\Delta/\Delta}$ mice having a better preserved capacity for acquiring new spatial memory.

We next assessed the balance and coordination using a Rotarod apparatus. We noted no difference in this functional parameter between young WT and mTOR$^{\Delta/\Delta}$ mice (Figure 4C). When compared to young WT mice, older WT mice were unable to remain as long on the spinning Rotarod apparatus. This is again consistent with the known decrement in balance and coordination as mice age (Barreto et al., 2010). Again, this decline in performance was significantly less marked in the mTOR$^{\Delta/\Delta}$ mice (Figures 4C and S4A). We observed a similar pattern when we assessed gait parameters of the mice. Stride width variability has been closely associated with falls in the elderly population (Hausdorff et al., 2001; Maki, 1997). Again, this parameter was similar in our cohorts of young WT and mTOR$^{\Delta/\Delta}$ mice (Figure 4D). As WT mice aged, stride width variability, an integrative measure

Cell PRESS
Open ACCESS

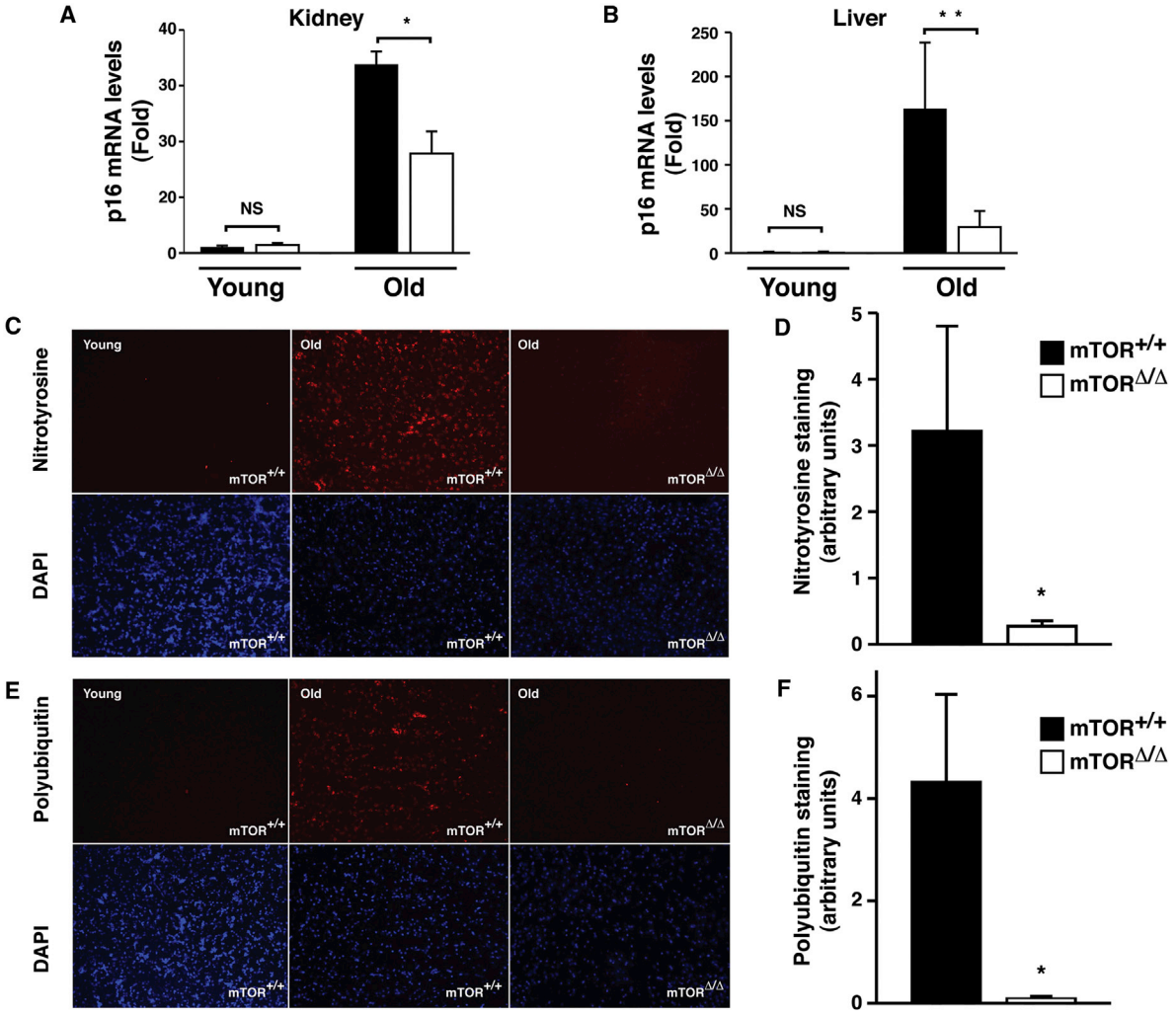

Figure 3. Molecular and Biochemical Biomarkers of Aging Are Reduced in Old mTOR$^{\Delta/\Delta}$ Mice

(A) Assessment of the age-dependent increase in kidney mRNA levels for the cell cycle inhibitor p16^{INK4a} normalized to GAPDH expression (n = three mice per genotype and age, with each mouse performed in triplicate).

(B) A similar assessment in old and young liver samples (n = six young WT and n = five young mTOR$^{\Delta/\Delta}$ samples; n = four old WT and n = four old mTOR$^{\Delta/\Delta}$ samples, with each sample performed in triplicate).

(C) Representative brain sections stained for nitrotyrosine (red, upper panels) obtained from young WT mice, old WT mice, and old mTOR$^{\Delta/\Delta}$ mice. Cell nuclei with stained concurrently with DAPI (blue, lower panels).

(D) Intensity of nitrotyrosine staining in the brains of old WT mice (n = three mice, with three to five determinations per mouse) and mTOR$^{\Delta/\Delta}$ mice (n = four mice, with three to five determinations per mouse).

(E) Staining for polyubquitinated proteins in brain tissue sections obtained from young WT mice, old WT mice, and old mTOR$^{\Delta/\Delta}$ mice. Upper panels (red) are stained with an antibody that recognizes proteins that are polyubiquitinated, and lower panels are analyzed by nuclear DAPI staining.

(F) Quantification of polyubiquitinated protein levels in brain sections of WT mice (n = three mice, with three to five determinations per mouse) and mTOR$^{\Delta/\Delta}$ mice (n = four mice, with three to five determinations per mouse).

All pooled data are presented as mean ± SEM. *$p < 0.05$. **$p < 0.01$. See also Figure S3.

of neurological, muscular, and postural control, increased. Again, this change was less evident in mTOR$^{\Delta/\Delta}$ mice (Figure 4D). Similarly, assessment of grip strength, a measure of muscle strength, demonstrated that, once again, mTOR$^{\Delta/\Delta}$ mice were protected from an age-dependent decline in function (Figure 4E).

While the mTOR$^{\Delta/\Delta}$ mice appeared to have slower decline in various age-dependent parameters, this was not universally true. Measurement of bone volume revealed that the age-dependent decrease in trabecular bone volume was actually more pronounced in the mTOR$^{\Delta/\Delta}$ mice (Figure 4F). Similarly, we noted that mTOR hypomorphic mice suffered a significant increase in the age-dependent increase in infections that predominantly affected the mouth, eye, and skin (Figure 4G). Thus, it appears that, in contrast to the other functional parameters measured, the age-dependent decline in bone volume and immune function were seemingly exacerbated in the mTOR$^{\Delta/\Delta}$ mice.

Cell PRESS
Open ACCESS

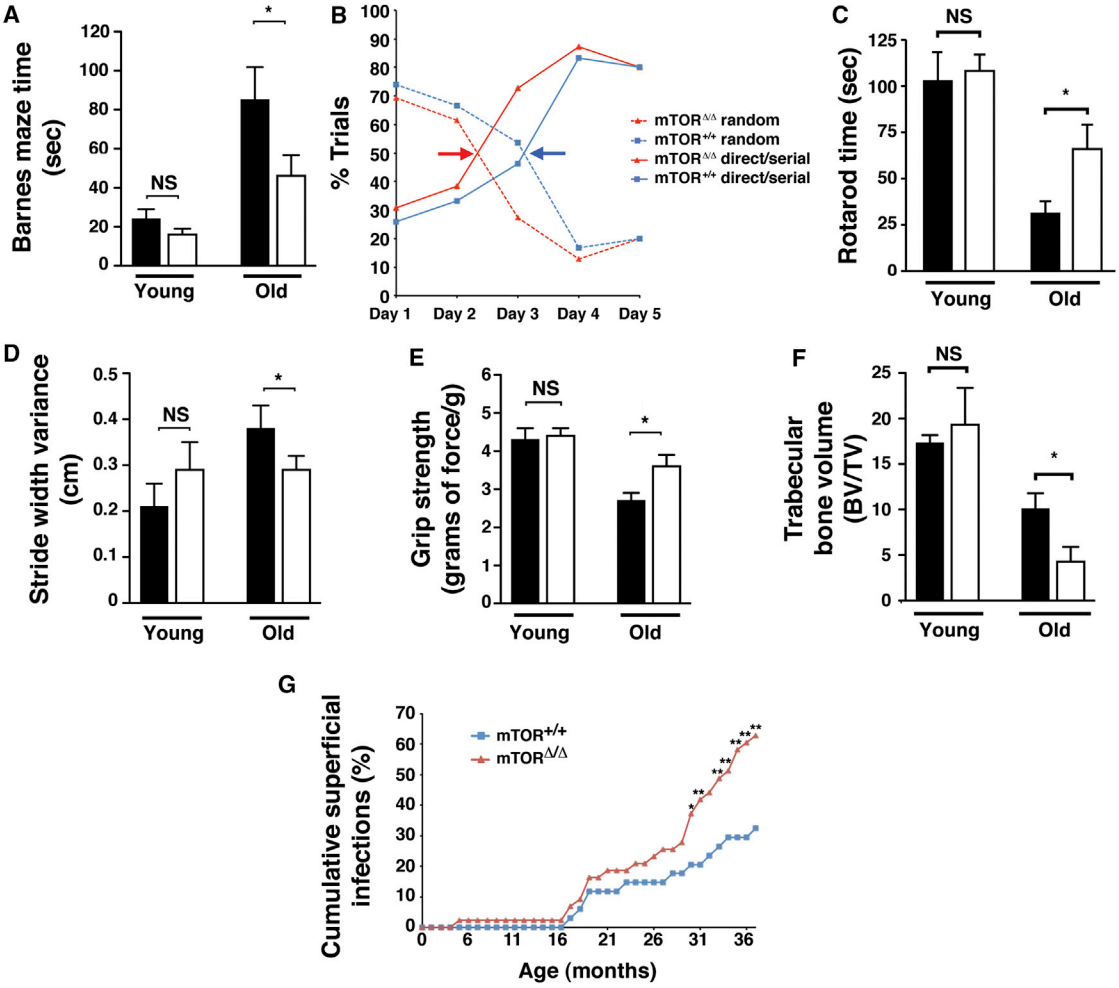

Figure 4. The Effects of Reduced mTOR Expression on a Range of Tissue Specific Age-Related Parameters

(A) Escape latency times on day 3 of training for the Barnes maze test for both young female (n = six mice per genotype) and old female (n = nine WT and n = 13 mTOR$^{\Delta/\Delta}$) mice. WT mice are represented by the shaded bars, while the open bars represent mTOR$^{\Delta/\Delta}$ mice. *$p < 0.05$.

(B) Learning strategy of old mice in the acquisition phase for training in the Barnes maze. Arrows indicate transition point between random to directed searching, an indicator of the speed in which new spatial learning is obtained (n = nine WT female mice, and n = 13 mTOR$^{\Delta/\Delta}$ female mice).

(C) Duration on the Rotarod, a measure of coordination and balance (n = six male mice per genotype for young mice; n = four old male WT, and n = seven old male mTOR$^{\Delta/\Delta}$ mice). *$p < 0.05$.

(D) Stride width variance in young (n = six young female mice per genotype) and old mice (n = six old WT male and female mice, and n = 13 old male and female mTOR$^{\Delta/\Delta}$ mice). *$p < 0.05$.

(E) Grip strength, normalized to gram of body weight, in young female mice (n = six per genotype) and old female mice (n = four WT mice, and n = 11 mTOR$^{\Delta/\Delta}$ mice). *$p < 0.05$.

(F) Assessment of the age-dependent decline in bone volume (BV) to tissue volume (TV) (n = four young mice per genotype, and n = six old mice per genotype). *$p < 0.05$.

(G) Age-dependent incidence of visibly apparent superficial infections of the skin, eyes, or mouth of the total cohort of WT and mTOR$^{\Delta/\Delta}$ mice (n = 34 WT mice, and n = 43 mTOR$^{\Delta/\Delta}$ mice; statistical analysis by Fisher's exact test). *$p < 0.05$. **$p < 0.01$.

All bar graph data are presented as mean ± SEM. See also Figure S4.

DISCUSSION

In summary, we describe a genetic model for reduced mTOR expression and activity that results in a robust increase in lifespan. The magnitude of lifespan extension in our model was larger than previously observed when mice were given rapamycin (Harrison et al., 2009). There are numerous possibilities that might explain these differences. First, in the initial report using rapamycin, the drug was initiated at 20 months of age. This contrasts with our model in which our genetic reduction of mTOR activity begins in the embryo. Indeed, a subsequent study, in which rapamycin was initiated at 9 months of age, saw slightly larger effects on lifespan (Miller et al., 2011). Another possibility is that the reduction in mTOR activity was greater in our model than can be achieved in animals treated pharmacologically. It should be noted that, while mTOR$^{\Delta/\Delta}$

Cell PRESS
Open ACCESS

mice were viable, when we bred mTOR$^{+/\Delta}$ mice, we consistently generated less than 25% of pups that were mTOR$^{\Delta/\Delta}$. This suggests that the reduction in mTOR expression we observed is close to what may be the lower limit needed for embryonic viability. Another possibility is that rapamycin is primarily an inhibitor of mTORC1 activity, although, as noted, with chronic administration it can have effects on mTORC2 activity as well (Lamming et al., 2012; Sarbassov et al., 2006). In contrast, our model leads to a balanced reduction in both mTORC1 and mTORC2 activity. Finally, it is important to note that we were dealing with a relatively small cohort of mice and that the observed median survival of our WT mice cohort (26.2 months) is on the short end of the published spectrum. As such, the precise magnitude of lifespan extension seen with the mTOR$^{\Delta/\Delta}$ mice must be viewed with caution until it is replicated in other facilities.

Our data suggest that a number of molecular, biochemical, and functional parameters of aging were reduced or slowed in the mTOR$^{\Delta/\Delta}$ mice. This is consistent with the notion that reducing mTOR expression does indeed slow the entire aging process in mammals (Wilkinson et al., 2012). Of note, our data clearly indicate that not all age-related parameters are regulated in an mTOR-dependent fashion. While the age-dependent increase in infection observed in mTOR$^{\Delta/\Delta}$ mice are likely related to the known role of mTOR in immune function (Chi, 2012; Zhang et al., 2011), these immune effects are less likely to explain the observed accelerated decline in bone volume in mTOR$^{\Delta/\Delta}$ mice. Perhaps more relevant is a set of recent observations suggesting a role for mTOR in modulating the age-dependent decline in bone mass (Xian et al., 2012). Finally, recent data suggest that long-term rapamycin treatment may accelerate cataract formation and augment testicular degeneration (Wilkinson et al., 2012). While these parameters were not part of our standard necropsy analysis, we did a separate analysis for a limited number of WT and mTOR$^{\Delta/\Delta}$ mice. While we saw no evidence for alterations in the testes (Figures S4B and S4C), our preliminary data are consistent with a potential role for mTOR activity in delaying cataract formation (Figure S4D).

Taken together, our observations suggest that single individual genetic pathways that extend lifespan will likely have nonuniform effects on the rate that individual tissues manifest their age-dependent decline in function. One interpretation of these observations would be that tissue aging and organismal aging are governed by interconnected but separable regulatory control mechanisms. One potential analogy might be circadian rhythms, whereby multiple distinct and independent peripheral clocks coexist in a confederation with a stronger central clock. In a similar fashion, our data suggest the interesting possibility that the rate of tissue aging may be viewed as influenced by, but not completely subservient to, the rate of organismal aging. Alternatively, our results could suggest the possibility that some interventions that slow aging may also have unintended, negative tissue-specific side effects. A very relevant precedent perhaps already exists for this phenomenon, as people who undergo voluntary caloric restriction appear to have a corresponding reduction in their bone mineral density (Villareal et al., 2011). Further analysis of this and related genetic models should help distinguish between these possibilities and, we hope, will help guide potential therapies aimed at extending lifespan and health span in people.

EXPERIMENTAL PROCEDURES

Mice

The generation of mTOR$^{\Delta/\Delta}$ mice has been previously described (Zhang et al., 2011). mTOR$^{\Delta/+}$ mice were crossed to generate mTOR$^{+/+}$ and mTOR$^{\Delta/\Delta}$ littermate mice used for this study. Mice were a mixed background consisting of 129S1 and C57BL/6Ncr strains. The proportion of mTOR$^{\Delta/\Delta}$ mice generated from parents bearing the mTOR$^{\Delta/+}$ genotype was less than the predicted 25% (97 mTOR$^{\Delta/\Delta}$ mice pups out of 697 live births, 13.9%), suggestive of some degree of embryonic lethality. All animal experiments were conducted in accordance with the guidelines of the Animal Care and Use Committee, National Heart, Lung and Blood Institute, National Institutes of Health (NIH). For genotype analysis, tissues were analyzed by PCR primers and conditions as described elsewhere (Zhang et al., 2011). Unless stated otherwise, young mice represent those that are between 3 and 6 months in age, and old mice represent those between 17 and 27 months in age. Specific ages, number, and sex of mice used varied and are listed under the relevant specific test.

Lifespan Analysis

For the determination of lifespan, male and female mTOR$^{+/+}$ and mTOR$^{\Delta/\Delta}$ mice were housed in a specific pathogen-free (SPF) facility. This means that mice entering the facility must be pathogen free with the exception of the specific pathogens *Helicobacter*, mouse parvovirus, or mouse norovirus. Mice were maintained in microisolator cages in ventilated racks with high-efficiency particulate air (or HEPA)-filtered supply and exhaust air. All cages were opened and changed inside biosafety cabinets or clean air hoods using microisolator technique. Mice were fed a regular chow diet consisting of 24% of calories derived from protein, 14% from fat, and 62% from carbohydrates (NIH-31/Harlan Teklad diet). Mice of different genotypes (mTOR$^{+/+}$ and mTOR$^{\Delta/\Delta}$ mice) were housed together, but male and female mice were maintained in separate cages. The maximum density was five mice per cage. The only withdrawal of mice from the study occurred within the first 6 months, when a limited number of WT and mTOR$^{\Delta/\Delta}$ male mice were excluded because of excessive fighting. Time of death is calculated using the date mice were found dead, or the time when the mice were determined to be moribund and/or displaying such severe discomfort that veterinary technicians recommended euthanasia. We sought to perform full autopsies on every mouse at the time of their withdrawal from the study; however, for various logistical reasons, a small fraction of mice of each genotype were not expeditiously forwarded to the pathologist (7 of 43 mTOR$^{\Delta/\Delta}$ mice and 8 of 34 WT mice). Pathological findings including malignant tumors were identified by a team of trained animal pathologists at a central core facility on the NIH Intramural campus. Mice involved in the lifespan analysis did not participate in any metabolic or physiological testing. Statistical analysis for the entire cohort used a Cox regression analysis using genotype and sex as parameters. The statistics for male and female survival was determined by the log rank test calculated by PRISM.

For additional details on the materials and methods used in this study, please see the Extended Experimental Procedures.

SUPPLEMENTAL INFORMATION

Supplemental Information includes Extended Experimental Procedures and four figures and can be found with this article online at http://dx.doi.org/10.1016/j.celrep.2013.07.030.

ACKNOWLEDGMENTS

We are grateful to Kumiko Torisu for helpful advice; Zu-Xi Yu for help with tissue sectioning; Lauren Brinster for animal pathology advice; William Jou and Tatyana Chanturiya for help with the metabolic testing; and David Allison, Timothy Mark Beasley, and John Dawson for statistical assistance. This work was supported by the NIH Intramural Research Program.

Cell PRESS
Open ACCESS

Received: February 14, 2013
Revised: July 11, 2013
Accepted: July 24, 2013
Published: August 29, 2013

REFERENCES

Barreto, G., Huang, T.T., and Giffard, R.G. (2010). Age-related defects in sensorimotor activity, spatial learning, and memory in C57BL/6 mice. J. Neurosurg. Anesthesiol. *22*, 214–219.

Bjedov, I., Toivonen, J.M., Kerr, F., Slack, C., Jacobson, J., Foley, A., and Partridge, L. (2010). Mechanisms of lifespan extension by rapamycin in the fruit fly Drosophila melanogaster. Cell Metab. *11*, 35–46.

Chi, H. (2012). Regulation and function of mTOR signalling in T cell fate decisions. Nat. Rev. Immunol. *12*, 325–338.

Cunningham, J.T., Rodgers, J.T., Arlow, D.H., Vazquez, F., Mootha, V.K., and Puigserver, P. (2007). mTOR controls mitochondrial oxidative function through a YY1-PGC-1alpha transcriptional complex. Nature *450*, 736–740.

Dazert, E., and Hall, M.N. (2011). mTOR signaling in disease. Curr. Opin. Cell Biol. *23*, 744–755.

Gangloff, Y.G., Mueller, M., Dann, S.G., Svoboda, P., Sticker, M., Spetz, J.F., Um, S.H., Brown, E.J., Cereghini, S., Thomas, G., and Kozma, S.C. (2004). Disruption of the mouse mTOR gene leads to early postimplantation lethality and prohibits embryonic stem cell development. Mol. Cell. Biol. *24*, 9508–9516.

Guertin, D.A., Stevens, D.M., Thoreen, C.C., Burds, A.A., Kalaany, N.Y., Moffat, J., Brown, M., Fitzgerald, K.J., and Sabatini, D.M. (2006). Ablation in mice of the mTORC components raptor, rictor, or mLST8 reveals that mTORC2 is required for signaling to Akt-FOXO and PKCalpha, but not S6K1. Dev. Cell *11*, 859–871.

Harrison, D.E., Strong, R., Sharp, Z.D., Nelson, J.F., Astle, C.M., Flurkey, K., Nadon, N.L., Wilkinson, J.E., Frenkel, K., Carter, C.S., et al. (2009). Rapamycin fed late in life extends lifespan in genetically heterogeneous mice. Nature *460*, 392–395.

Hausdorff, J.M., Rios, D.A., and Edelberg, H.K. (2001). Gait variability and fall risk in community-living older adults: a 1-year prospective study. Arch. Phys. Med. Rehabil. *82*, 1050–1056.

Kaeberlein, M., Powers, R.W., 3rd, Steffen, K.K., Westman, E.A., Hu, D., Dang, N., Kerr, E.O., Kirkland, K.T., Fields, S., and Kennedy, B.K. (2005). Regulation of yeast replicative lifespan by TOR and Sch9 in response to nutrients. Science *310*, 1193–1196.

Kapahi, P., Zid, B.M., Harper, T., Koslover, D., Sapin, V., and Benzer, S. (2004). Regulation of lifespan in Drosophila by modulation of genes in the TOR signaling pathway. Curr. Biol. *14*, 885–890.

Kastle, M., and Grune, T. (2011). Protein oxidative modification in the aging organism and the role of the ubiquitin proteasomal system. Curr. Pharm. Des. *17*, 4007–4022.

Kennard, J.A., and Woodruff-Pak, D.S. (2011). Age sensitivity of behavioral tests and brain substrates of normal aging in mice. Front Aging Neurosci *3*, 9.

Kenyon, C. (2011). The first long-lived mutants: discovery of the insulin/IGF-1 pathway for ageing. Philos. Trans. R. Soc. Lond. B Biol. Sci. *366*, 9–16.

Krishnamurthy, J., Torrice, C., Ramsey, M.R., Kovalev, G.I., Al-Regaiey, K., Su, L., and Sharpless, N.E. (2004). Ink4a/Arf expression is a biomarker of aging. J. Clin. Invest. *114*, 1299–1307.

Lamming, D.W., Ye, L., Katajisto, P., Goncalves, M.D., Saitoh, M., Stevens, D.M., Davis, J.G., Salmon, A.B., Richardson, A., Ahima, R.S., et al. (2012). Rapamycin-induced insulin resistance is mediated by mTORC2 loss and uncoupled from longevity. Science *335*, 1638–1643.

Laplante, M., and Sabatini, D.M. (2012). mTOR signaling in growth control and disease. Cell *149*, 274–293.

Maki, B.E. (1997). Gait changes in older adults: predictors of falls or indicators of fear. J. Am. Geriatr. Soc. *45*, 313–320.

Medvedik, O., Lamming, D.W., Kim, K.D., and Sinclair, D.A. (2007). MSN2 and MSN4 link calorie restriction and TOR to sirtuin-mediated lifespan extension in Saccharomyces cerevisiae. PLoS Biol. *5*, e261.

Miller, R.A., Harrison, D.E., Astle, C.M., Baur, J.A., Boyd, A.R., de Cabo, R., Fernandez, E., Flurkey, K., Javors, M.A., Nelson, J.F., et al. (2011). Rapamycin, but not resveratrol or simvastatin, extends lifespan of genetically heterogeneous mice. J. Gerontol. A Biol. Sci. Med. Sci. *66*, 191–201.

Murakami, M., Ichisaka, T., Maeda, M., Oshiro, N., Hara, K., Edenhofer, F., Kiyama, H., Yonezawa, K., and Yamanaka, S. (2004). mTOR is essential for growth and proliferation in early mouse embryos and embryonic stem cells. Mol. Cell. Biol. *24*, 6710–6718.

Sarbassov, D.D., Ali, S.M., Sengupta, S., Sheen, J.H., Hsu, P.P., Bagley, A.F., Markhard, A.L., and Sabatini, D.M. (2006). Prolonged rapamycin treatment inhibits mTORC2 assembly and Akt/PKB. Mol. Cell *22*, 159–168.

Schöneich, C. (2006). Protein modification in aging: an update. Exp. Gerontol. *41*, 807–812.

Selman, C., Tullet, J.M., Wieser, D., Irvine, E., Lingard, S.J., Choudhury, A.I., Claret, M., Al-Qassab, H., Carmignac, D., Ramadani, F., et al. (2009). Ribosomal protein S6 kinase 1 signaling regulates mammalian lifespan. Science *326*, 140–144.

Shang, F., and Taylor, A. (2011). Ubiquitin-proteasome pathway and cellular responses to oxidative stress. Free Radic. Biol. Med. *51*, 5–16.

Vellai, T., Takacs-Vellai, K., Zhang, Y., Kovacs, A.L., Orosz, L., and Müller, F. (2003). Genetics: influence of TOR kinase on lifespan in C. elegans. Nature *426*, 620.

Villareal, D.T., Kotyk, J.J., Armamento-Villareal, R.C., Kenguva, V., Seaman, P., Shahar, A., Wald, M.J., Kleerekoper, M., and Fontana, L. (2011). Reduced bone mineral density is not associated with significantly reduced bone quality in men and women practicing long-term calorie restriction with adequate nutrition. Aging Cell *10*, 96–102.

Wang, C., Li, Q., Redden, D.T., Weindruch, R., and Allison, D.B. (2004). Statistical methods for testing effects on "maximum lifespan". Mech. Ageing Dev. *125*, 629–632.

Wilkinson, J.E., Burmeister, L., Brooks, S.V., Chan, C.C., Friedline, S., Harrison, D.E., Hejtmancik, J.F., Nadon, N., Strong, R., Wood, L.K., et al. (2012). Rapamycin slows aging in mice. Aging Cell *11*, 675–682.

Xian, L., Wu, X., Pang, L., Lou, M., Rosen, C.J., Qiu, T., Crane, J., Frassica, F., Zhang, L., Rodriguez, J.P., et al. (2012). Matrix IGF-1 maintains bone mass by activation of mTOR in mesenchymal stem cells. Nat. Med. *18*, 1095–1101.

Zhang, S., Readinger, J.A., DuBois, W., Janka-Junttila, M., Robinson, R., Pruitt, M., Bliskovsky, V., Wu, J.Z., Sakakibara, K., Patel, J., et al. (2011). Constitutive reductions in mTOR alter cell size, immune cell development, and antibody production. Blood *117*, 1228–1238.

Zoncu, R., Efeyan, A., and Sabatini, D.M. (2011). mTOR: from growth signal integration to cancer, diabetes and ageing. Nat. Rev. Mol. Cell Biol. *12*, 21–35.